

## Analysis of tissue flow patterns during primitive streak formation in the chick embryo

Cheng Cui<sup>a</sup>, Xuesong Yang<sup>b</sup>, Manli Chuai<sup>b</sup>, James A. Glazier<sup>a</sup>, Cornelis J. Weijer<sup>b,\*</sup>

<sup>a</sup>Department of Physics, Biocomplexity Institute, Indiana University, 727 East Third Street, Swain Hall West 159, Bloomington, IN 47405-7105, USA

<sup>b</sup>Division of Cell and Developmental Biology, Wellcome Trust Biocentre, School of Life Sciences, University of Dundee, Dundee DD1 5EH, UK

Received for publication 28 October 2004, revised 19 February 2005, accepted 8 April 2005

Available online 13 June 2005

### Abstract

We have investigated the patterns of tissue flow underlying the formation of the primitive streak in the chick embryo. Analysis of time-lapse sequences of brightfield images to extract the tissue velocity field and of fluorescence images of small groups of DiI-labelled cells have shown that epiblast cells move in two large-scale counter-rotating streams, which merge at the site of streak formation. Despite the large-scale tissue flows, individual cells appear to move little relative to their neighbours. As the streak forms, it elongates in both the anterior and posterior directions. Inhibition of actin polymerisation via local application of the inhibitor latrunculin A immediately terminates anterior extension of the streak tip, but does not prevent posterior elongation. Inhibition of actin polymerisation at the base of the streak completely inhibits streak formation, implying that continuous movement of cells into the base of the forming streak is crucial for extension. Analysis of cycling cells in the early embryo shows that cell-cycle progression in the epiblast is quite uniform before the primitive streak forms then decreases in the central epiblast and incipient streak and increases at the boundary between the *area pellucida* and *area opaca* during elongation. The cell-cycle inhibitor aphidicolin, at concentrations that completely block cell-cycle progression, permits initial streak formation but arrests development during extension. Our analysis suggests that cell division maintains the cell-flow pattern that supplies the streak with cells from the lateral epiblast, which is critical for epiblast expansion in peripheral areas, but that division does not drive streak formation or the observed tissue flow.

© 2005 Published by Elsevier Inc.

**Keywords:** Primitive streak; Cell movement; Cell proliferation; FGF signalling; Time-lapse analysis; Vector velocity field

### Introduction

The formation of the primitive streak is one of the most striking phenomena in the early development of the chick embryo. The streak forms from epiblast cells overlying Koller's sickle. It first becomes visible as an accumulation of cells at the posterior pole of the epiblast then extends anteriorly for up to 12 h until it reaches a length of 80% of the extension of the epiblast, after which it starts to regress (Bachvarova et al., 1998). The streak is the site of the dorso-ventral ingression of mesoderm and endoderm cells. Extensive recent fate-map studies using localised injection of the lipophilic dye DiI have clarified the fate of cells in the

epiblast (Hatada and Stern, 1994). Time-lapse analyses of embryos labelled with iron and carbon particles performed more than 70 years ago suggested that streak formation involved large-scale movement of cells from the sickle into the streak (Graeper, 1929; Vakaet, 1970). Graeper noted that, during streak formation, cells from the lateral posterior marginal zone move towards the centre of the marginal zone where they merge and extend anteriorly, forming a "Doppelwirbel" which he named *polonaise* movements. More recent experiments, which labelled groups of cells in different positions with DiI and followed their fate over time, showed that sickle cells move to occupy a range of anterior–posterior positions in the streak (Lawson and Schoenwolf, 2001). Cells in Koller's sickle express a characteristic set of genes that play important roles in the control of later development, e.g. signalling molecules of

\* Corresponding author. Fax: +44 1382 345386.

E-mail address: [c.j.weijer@dundee.ac.uk](mailto:c.j.weijer@dundee.ac.uk) (C.J. Weijer).

the FGF and TGF- $\beta$  families as well as cell-type-specific transcription factors (Chapman et al., 2002, 2004; Lawson et al., 2001). The expression domain of these genes conformally transforms from a sickle-shaped domain via an intermediate triangular shape into an elongated domain along the midline of the embryo, stretching in an anterior direction from the posterior marginal zone. The primitive streak forms along the embryo midline. This coordinated change in gene expression pattern also suggests that the initially sickle-shaped group of cells transforms into the streak by rearrangement of the cells along the midline of the embryo. Recent insights into the mechanisms controlling streak induction include the observations that misexpression of the TGF- $\beta$  family member Vg1, which normally expresses in the posterior marginal zone, can induce ectopic primitive streaks and that Vg1 requires the expression of Wnt8 to exert its effects (Shah et al., 1997; Skromne and Stern, 2001, 2002). The hypoblast also seems important in controlling streak formation, secreting a nodal antagonist needed to suppress ectopic streaks (Bertocchini and Stern, 2002). Rotation of the hypoblast can bend the forming streak (Foley et al., 2000; Waddington, 1932, 1933).

Despite considerable progress in understanding the signalling pathways controlling streak formation, the cellular mechanisms underlying the observed cell behaviours have remained elusive. The rapid growth of the embryo during early development requires extensive cell division, e.g. in the fully extended streak (HH 4–5) stages (Sanders et al., 1993). We generally lack data on cell division patterns before and during the initial stages of streak formation. Descendants of cells transfected with a *lacZ*-expressing retrovirus can form strings of cells aligned along the anterior–posterior axis of the forming streak, suggesting that streak formation and/or extension could result from successive, oriented cell divisions, with mitotic spindles aligned along the anterior–posterior axis of the embryo (Wei and Mikawa, 2000). Adams and coworkers have also observed oriented cell cleavage and movement during zebrafish embryo gastrulation but found no strong correlation between the plane of cell division and the direction of movement (Concha and Adams, 1998; Gong et al., 2004).

In this paper, we characterise tissue movement in the epiblast quantitatively, using specialised image-processing techniques to extract local, flow-velocity fields from time-lapse sequences of brightfield images of early chick development. We also track several small groups of DiI-labelled cells in the epiblast during streak development. These measurements confirm that, during streak formation, cells flow from the posterior sickle towards the posterior midline where they meet and extend anteriorly in a polonaise movement. We extend these observations to show that these movements are part of two large-scale counter-rotating tissue flows forming closed loops around two stationary centres. Furthermore, the posterior extension of the embryo starts before the streak becomes visible as a distinct structure. To address the role of cell division in

streak formation, we characterised the pattern of cell-cycle progression by measuring the relative distribution of S phase cells. These observations show that cycling cells are distributed more or less randomly in the early epiblast but that, during streak formation, the majority of cycling cells lie in a boundary region between the *area pellucida* and *area opaca*, suggesting that cell division may help to drive the tissue flows. Arresting cells in S phase by applying the DNA polymerase inhibitor aphidicolin severely impeded development but did not inhibit cell flows during the initial stages of streak formation, indicating that streak initiation does not require cell division.

## Materials and methods

### *Embryo culture*

We incubated fertilised white leghorn eggs (High Sex  $\times$  Rhode Island Red; Winter Farm, Thirplow, Herts, UK) at 37°C for 0–8 h to obtain embryos between Eyal-Giladi and Kochav stage-X and HH stage 1 (Eyal-Giladi and Kochav, 1976; Hamburger and Hamilton, 1992). We cultured the embryos using the EC culture technique, which uses a filter paper carrier to hold the early blastoderm and vitelline membranes under tension while the embryo grows on a substratum of agar-albumen, exactly as described (Chapman et al., 2001). We removed any extra yolk cells floating on top of the *area pellucida* using fine-tip forceps to improve our view of the *area pellucida* when injecting DiI and acquiring images.

### *Cell tracking with DiI and time-lapse microscopy*

We used the carbocyanine dye 1,1'-dioctadecyl-3,3,3',3'-tetramethyl indocarbocyanine perchlorate (*DiI*) (Molecular Probes, Inc.) to label small groups of cells. We diluted a 2.5% stock of DiI in ethanol 1:10 in 0.3 M sucrose at 45°C and injected it into the epiblast layer by air pressure through a micropipette pulled from a 1 mm glass capillary in a vertical micropipette puller (Sutter Inc. model P-30). Normally, each labelled group contained 10–30 cells. We incubated the labelled embryo in a purpose built incubation chamber (20  $\times$  20  $\times$  6 cm) heated to 37°C by blowing through humidified air, heated with an Air Therm heating unit (World Precision Instruments) mounted on the stage of an inverted microscope (Zeiss Axiovert 135TV). Fluorescent and brightfield images were taken every 4 min for 12–15 h, using a cooled CCD camera (Hamamatsu 4770). We processed the resulting images using Matlab routines and compressed them into MPEG4 movies.

### *Application of latrunculin A*

We implanted beads soaked in the actin polymerisation inhibitor latrunculin A in embryos of various stages to

interfere with actin-driven cell movement. We dissolved the latrunculin A to a concentration of 40  $\mu\text{M}$  in DMSO. We prepared Dowex AG1 X8 ion exchange beads by washing them in PBS and incubating them in the latrunculin solution for 1 h. We then washed the beads three times for 5 min in PBS and implanted them at different positions in the embryos and made time-lapse videos of the resulting development.

#### *Application of aphidicolin to block cell division*

We applied solutions of aphidicolin of different concentrations to the top of the chick embryo cultures after DiI injection. As a control, we treated other embryos with the same volume of PBS. We made both fluorescent and brightfield movies of the aphidicolin-treated embryos as described above and processed the images to calculate cell trajectories.

#### *8-Bromo-deoxy-uridine incorporation and immunohistochemistry*

We incubated eggs for 8 h at 38°C to HH stage 1. We transferred the embryos to EC cultures and incubated them with 100  $\mu\text{l}$  of 10  $\mu\text{M}$  BrdU in PBS (PharMingen Cat No. 2420KC) for 2 h (Wei and Mikawa, 2000). To block S phase progression, we treated the embryos with aphidicolin (20  $\mu\text{l}$  of 10  $\mu\text{M}$  solution or 10  $\mu\text{l}$  of 100  $\mu\text{M}$  solution). To stain for BrdU incorporation, we fixed the embryos in 4% paraformaldehyde at 4°C overnight. After washing the fixed embryos with TBST for 30 min, we incubated them in 2 M HCl for 60 min to denature the DNA. We then washed them three times with TBST and incubated them with anti-BrdU (PharMingen, Cat No. 555627 1:200, diluted with 1% BSA/PBS) antibody for 24 h at 4°C. After washing them with TBST three times, we incubated them with HRP conjugated anti-mouse antibody (Promega, 1:200 diluted 1% BSA/PBS) for 20 h at 4°C followed by three washes with TBST. To develop the BrdU pattern, we first incubated the embryos in DAB/Tris for 30 min at room temperature in the dark then in DAB/Tris containing 0.3 mM  $\text{H}_2\text{O}_2$  for 5 min at room temperature. Finally, we washed them in PBS containing 2 mM  $\text{NaN}_3$  to stop development, cut them from the vitelline membrane and surrounding yolk cells, and mounted them on slides in 50 mM TRIS/HCl (pH7.5) containing 80% glycerine.

#### *Image analysis*

We calculated cell trajectories from the information in successive time-lapse images using routines written in the Optimas VI (Media Cybernetics) macro language (see Yang et al., 2002). We extracted the velocity vector fields using a dedicated C programme, which calculates the information flow for every pixel in the image and displays it in various ways. For details on the theory

and application of this method to tissue movements in *Dictyostelium* mounds and slugs, see Siegert et al. (1994).

## **Results**

To quantitatively analyse tissue movements during streak formation, we processed time series of brightfield images of developing chick embryos in EC culture to obtain vector velocity fields for of the entire epiblast. We combined this information with DiI labelling of small groups of cells in the epiblast, which reveals the movement of small groups of cells. We then used tracking algorithms to visualise and measure the movement of these cells before and during streak formation and extension.

#### *Tissue movement patterns during streak formation*

To analyse tissue movement during streak formation, we DiI-labelled small groups of cells at multiple locations in a single embryo. We allowed these embryos to develop in EC culture and followed the movement of the labelled cells by time-lapse observation over the 10–15 h period of streak development. We collected both brightfield and fluorescence images at 4 min intervals for up to 15 h and followed the tissue movements during the early stages of streak formation. These labelled groups of cells showed two large-scale counter-rotating tissue flows in the epiblast, which merged at the site where the streak was going to form a few hours before the streak became visible as an optically dense structure (Fig. 1). Two areas of relatively little movement that did not coincide with any particular morphological structures or any known cell type formed the centres of both counter-rotating flows. Our DiI labelling experiments (Fig. 1) showed little relative cell movement despite large-scale cell displacements; the cells in labelled patches stayed close together. Closer inspection of the groups of labelled cells revealed that cells from individual patches split up into several smaller units, but we could not determine whether these splits were due to adjacent cells moving apart or cells dividing, or both.

Quantitative high-resolution analysis of brightfield images of tissue movements in the epiblast using optical flow detection confirmed the two counter-rotating flows (Figs. 2, 3). In the images, speeds vary from 0.1–1.5  $\mu\text{m}/\text{min}$  at different locations, with the highest speeds at the site of streak formation and the outer periphery of the flows. The large scale and symmetry of these flow patterns are remarkable. Cells, not only move vigorously from the sickle region towards the site of streak formation as Graeper described, but also anteriorly and laterally away from the site of streak formation, forming large-scale closed loop flows, which strongly resemble flows in fluids. We observed many embryos (>60) and always found the same flow patterns.



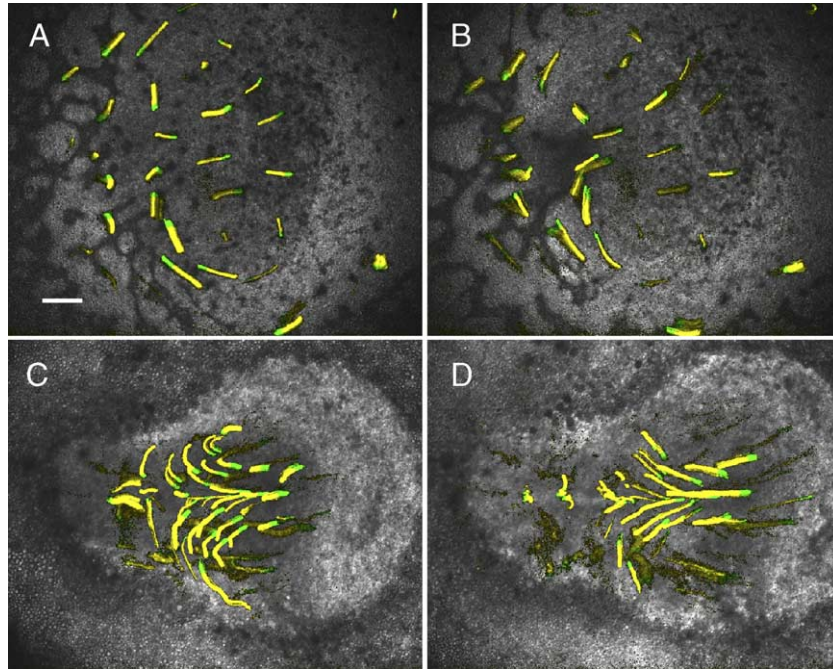


Fig. 1. Cell flow patterns revealed by DiI injection in an HH stage 1 and an HH stage 3 embryo. We labelled several small groups of cells in one embryo (HH stage 1) with DiI. We recorded brightfield and fluorescent images at 4 min intervals and calculated the tracks of the groups of DiI-labelled cells. (A, B) Brightfield images of the developing embryo 160 min and 480 min after the start of the recording overlaid with the tracks of cell movement. The tracks show movement of labelled cells in the last 160 min before we took the brightfield images, while the green heads of the tracks show movement of labelled cells in the last 40 min indicating the movement direction. (C, D) Brightfield images overlaid with tracks for an embryo labelled at HH stage 3. The scale bar in panel (A) is 250  $\mu\text{m}$ . See supplementary material for movie 1 and movie 2 showing the experiments shown in A, B and C, D, respectively.

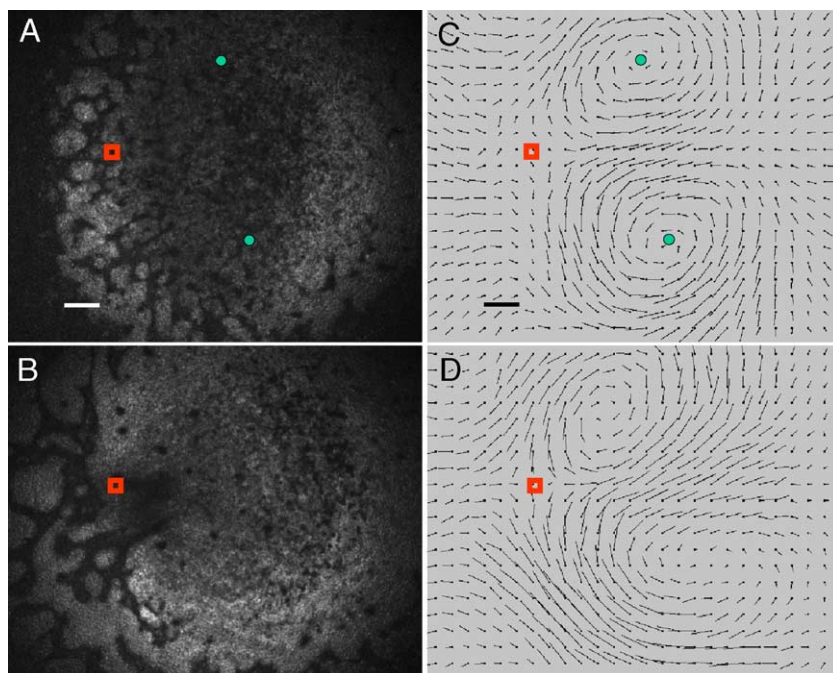


Fig. 2. Velocity vector fields of cells in the embryo during streak formation. (A, B) Brightfield images of the developing embryo shown in Fig. 3 at 40 min (before streak formation) and 320 min (after streak formation) after the start of the recording. (C, D) Corresponding velocity vector fields calculated over the last 10 consecutive images taken 4 min apart. The red box indicates the saddle-point area where the cell flows merge and bifurcate along the anterior–posterior axis. The green points in panels (A) and (C) indicate the quiescent points of low flow. The vectors show the average velocities calculated over 10 frames (40 min). The white scale bar in panel (A) is 250  $\mu\text{m}$ , the black scale bar in panel (C) represents a velocity of 1  $\mu\text{m}/\text{min}$ . See supplementary material movie 3 for a dynamic presentation of this experiment.

Our experiments also showed clearly that the cells flowing towards the streak bifurcate into two streams that flow, either anteriorly (contributing to the anterior elongation of the streak) or posteriorly (contributing to the posterior extension of the streak). Thus, streak elongation is bidirectional from its initiation. We mark this bifurcation point with a small red box in our velocity-field figures (Figs. 2, 3). During streak elongation, this bifurcation point seems to move anteriorly relative to the length of the streak until, at the extended streak (HH stage 4) stage, this point lies almost in the middle of the streak (Fig. 3), while the embryo changes from a circle to a pear shape (Figs. 2, 3). These observations indicate a gradual increase in the rate of posterior extension relative to the rate of anterior extension. We do not know what determines this change in relative elongation rates. Possibly, proliferation is faster in the posterior epiblast than in the central epiblast (Figs. 5B, E) since elongation of the embryos did not occur in the presence of aphidicolin (Fig. 6).

*Streak formation and extension occur actively both at the base and tip of the streak*

The above observations demonstrate the large-scale connected flow of the tissue around two quiescent points in the lateral part of the epiblast but do not show which cells in the streak move actively. A control bead implanted at the tip of a forming streak (HH stage 2) remained localised at the tip of the streak when the streak elongated. The streak

tip pushed the bead forward, and all movements were normal (Figs. 4A, B, C). Thus, streak elongation is active and can push an inert object. How do these forces arise? We locally applied beads soaked in the actin polymerisation inhibitor latrunculin B at various positions in the streak (Fig. 4). Latrunculin slowly leaches off the beads to locally inhibit actin polymerisation and thus movement in cells that receive a high enough dose. This local inhibition of movement enables us to investigate the role of local cell movement on streak extension. Grafting a bead at the tip of the streak immediately inhibits extension of the streak in the anterior direction, that is, the tip of the streak no longer moves towards the anterior boundary of the embryo (Figs. 4D, E, F). However, closer observation revealed that the streak still elongates due to posterior extension of the streak, as is evident from the velocity flow field (compare flows in Figs. 4C and F). Implantation of latrunculin beads at the base of a forming streak blocks both anterior and posterior streak elongation almost completely (Figs. 4G, H, I), there is no significant elongation of the streak during the 6.5 h period of observation. The large outward directed velocity vectors in the periphery of the embryo reflect the growth of the embryo, which is not affected by the local application of latrunculin. These observations suggest that the majority of cells that contribute to the streak must move through the posterior area of the embryo and that this movement is active and actin-dependent, resulting either from cell division or crawling of cells on the basement membrane/extracellular matrix.

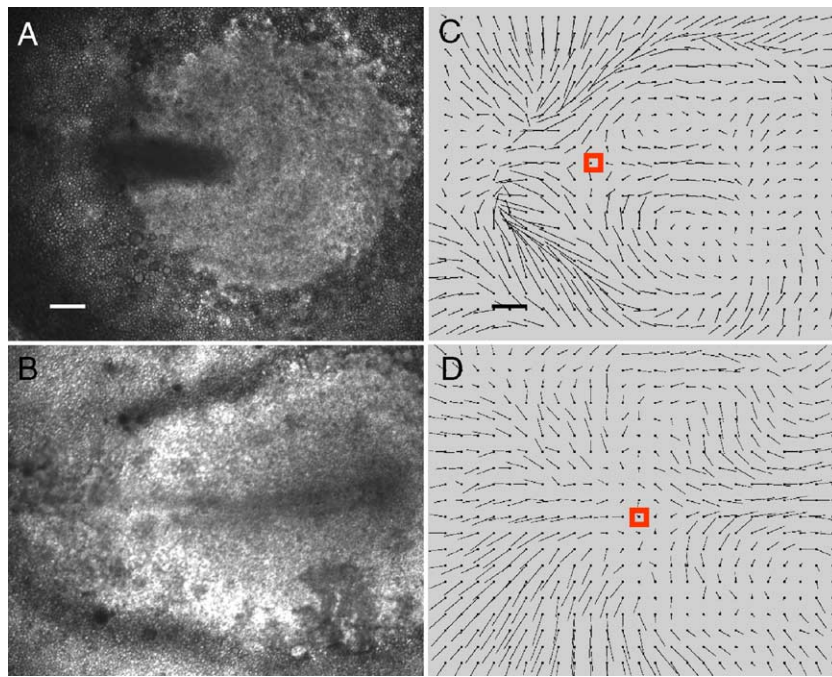


Fig. 3. Vector velocity field of epiblast movement during streak elongation. (A, B) Brightfield images of a developing embryo at different stages (at 40 min and 600 min after the start of the recording). (C, D) Corresponding velocity vector fields calculated over 10 consecutive images taken at 4 min intervals. Note the change in position of the bifurcation point (red box) where the cells divide into anterior-moving and posterior-moving streams. The white scale bar in panel (A) represents 500  $\mu\text{m}$ , the black scale bar in panel (C) represents a velocity of 1  $\mu\text{m}/\text{min}$ . See supplementary material movie 4 for a dynamic presentation of this experiment.



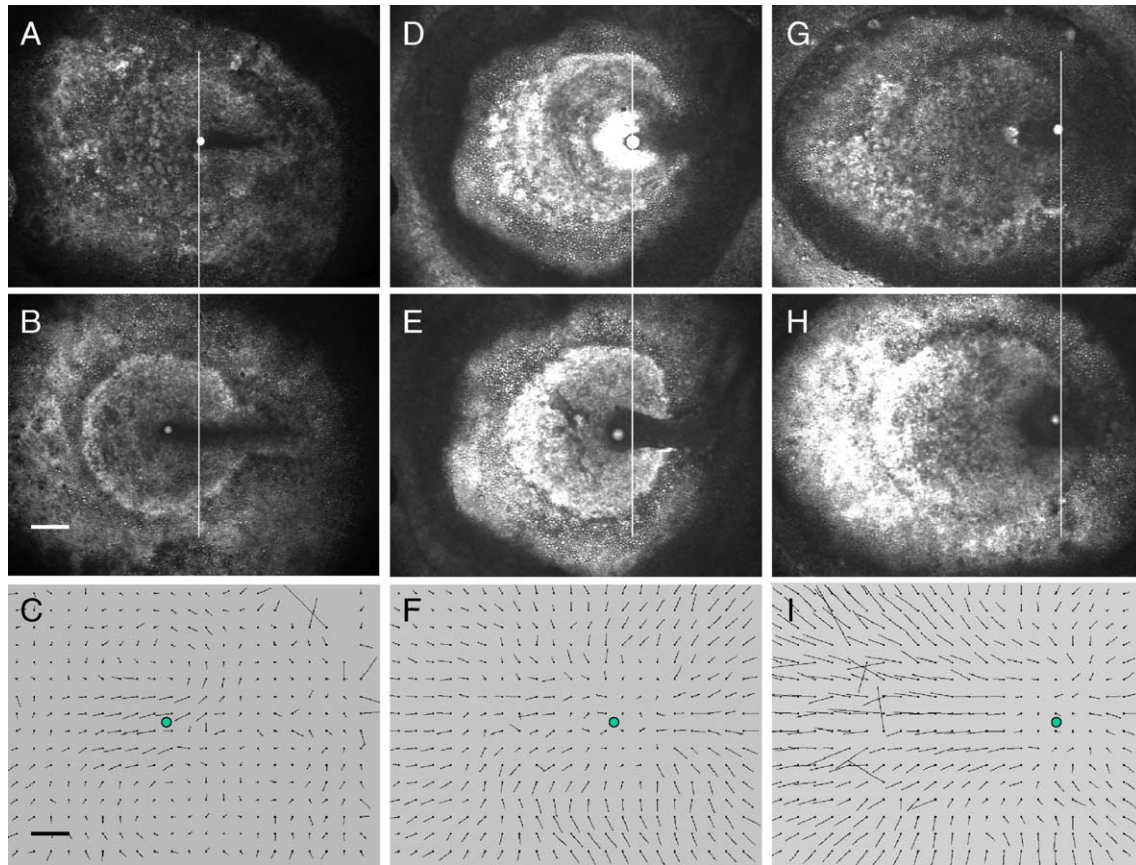


Fig. 4. Inhibition of streak extension by local inhibition of actin polymerisation. (A, B, C) Movement of a control bead implanted at the tip of the streak in an HH stage 2 embryo (A) and the same embryo 6.5 h later (B). (C) Tissue flow velocity field calculated over a 30 min period 6–6.5 h after implantation of the bead. (D, E, F) Embryo with a bead soaked in 40 mM latrunculin implanted at the tip of the streak at the start of the experiment (D) and the same embryo 6.4 h later (E). (F) Tissue flow velocity field calculated over a 30 min period 6–6.5 h after implantation of the bead. (G, H, I) Embryo with a latrunculin soaked bead implanted at the base of the forming streak at the start of the experiment (G) and 6.5 h after implantation (H). (I) Flow velocity field 6–6.5 h after implantation. Green circles in panels (C, F, I) correspond to the position of the beads at 6.5 h. The vertical line is drawn to aid in comparing the position of the bead at the start of the experiment with that after 6.5. The white scale bar in panel (B) represents 300  $\mu\text{m}$ , the black scale bar in panel (C) represents a velocity of 1  $\mu\text{m}/\text{min}$ . See supplementary material movies 5, 6, 7 for a dynamic representation of the experiments shown in A–C, D–F and G–I, respectively.

#### *The role of cell division in streak formation and elongation*

Experiments labelling individual cells with *lacZ*-expressing virus particles have shown that cells in the streak mostly divide with their cleavage plane perpendicular to the direction of streak elongation, giving rise to strings of cells aligned along the long axis of the streak (Wei and Mikawa, 2000). We cannot conclude whether oriented cell divisions drive or result from the cell flows. In the absence of quantitative information on cell division and cell-cycle progression before and during the early stages of streak formation, we investigated the pattern of cell-cycle progression in more detail. We located cells in S phase using a 2 h BrdU pulse labelling (Fig. 5). During early stages (HH 1–2), the BrdU incorporating cells in the epiblast showed no specific pattern, except that they concentrated at the outermost edge of the *area opaca*, which expands over the yolk as the embryo grows (Figs. 5A, D). In embryos labelled during the initial stages of streak formation, more cells in the region between the

*area opaca* and the *area pellucida* incorporated BrdU, while fewer cells in the central region of the embryo incorporated BrdU (Figs. 5B, E). To investigate whether these cell divisions form and elongate the streak, we incubated embryos with the DNA polymerase inhibitor aphidicolin. We used aphidicolin to block cell-cycle progression since, unlike most mitotic inhibitors, it does not directly interfere with the cytoskeleton (which would affect the cells' motile machinery). Control points which check for the successful replication of DNA before allowing cells to proceed into mitosis and cytokinesis allow blocking of DNA synthesis to indirectly block cell division (Michael and Newport, 1998). Incubation of our cells with aphidicolin completely inhibited BrdU incorporation, indicating effective cell-cycle arrest (Figs. 5C, F). In embryos receiving concentrations of aphidicolin that completely inhibited DNA replication, cells from the sickle region still moved towards the posterior midline, the position where the streak normally initiates, however, the streak did not extend completely, causing compaction

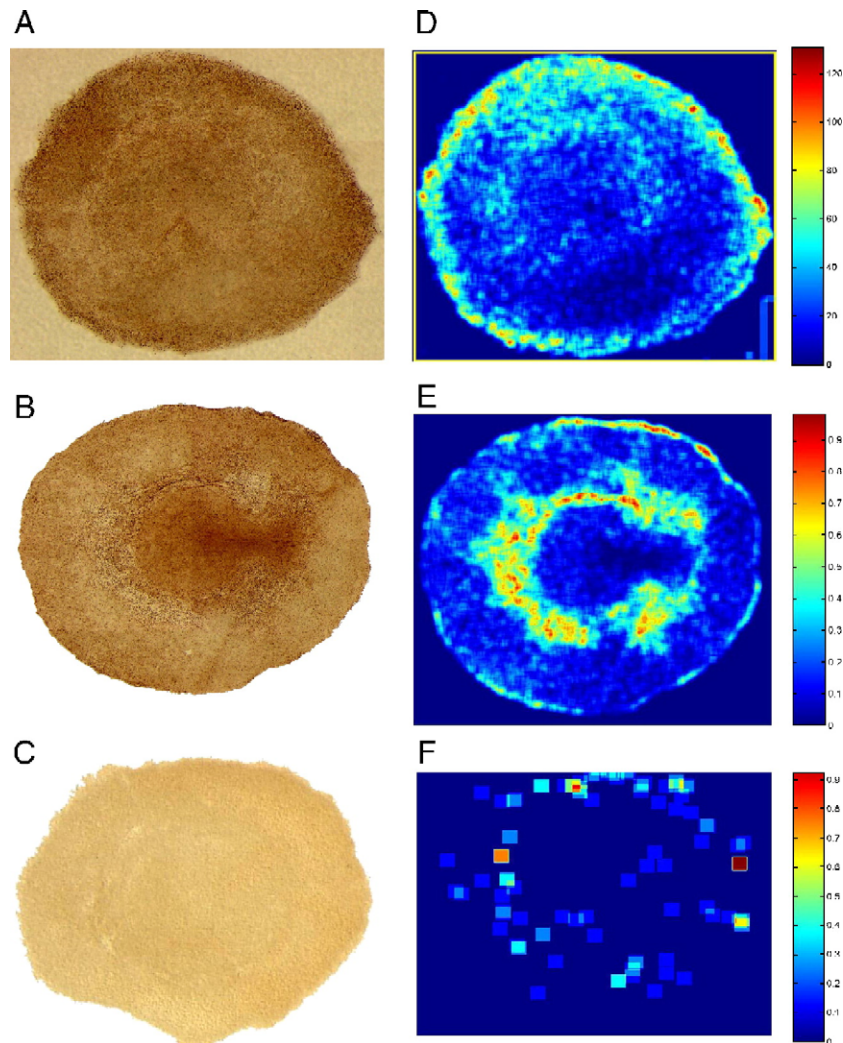


Fig. 5. Spatial distribution of cells in S phase during early development. (A) Prestreak embryo (HH stage 1) showing uniform labelling of cells in the epiblast, with a slightly higher degree of labelling at the outmost periphery of the embryo. (B) HH stage 3<sup>+</sup> embryo showing somewhat more labelling in the boundary region between the *area pellucida* and *area opaca*. (C) Complete inhibition of DNA synthesis in the presence of aphidicolin (10  $\mu$ l, 100  $\mu$ M). (D–F) The relative number of cells in S phase for images (A–C). We determined the number of cycling cells determined for a 25  $\times$  25 grid covering the images and displayed it as a relative colour map. After aphidicolin treatment (C), BrdU incorporation effectively ceases.

of cells and local increase in tissue density in this area. Cells located in the anterior and lateral parts of the *area pellucida* moved radially, directly towards the posterior pole, the site of streak formation, without following the normal circular flow patterns (Fig. 6), resulting in a large aggregation of cells at the site of streak formation. In all these experiments, the embryo tore itself apart, suggesting that the condensation of cells at the site of streak formation generates forces independent of cell division. Since cells initially aggregate at the site of streak formation in the absence of cell division, some other mechanisms must drive aggregation. Our analysis suggests that increased cell division in a region between the *area opaca* and *area pellucida* is necessary for proper cell movement during the later stages of streak formation, especially during and after the half-extended streak stage, when the cells start to invaginate in the streak and cells dividing in the

epiblast must replace the cells that disappear from the surface.

## Discussion

### *Streak formation involves large-scale, active tissue flows*

Our observations of the cell flow patterns do not indicate whether all or only some cells move actively. Since the cells in the epiblast form a tightly connected epithelial sheet, local movement of one group of cells requires other cells to rearrange in order to maintain the integrity of the epithelial sheet. In this sense, cell flow patterns very much resemble flow patterns in a fluid, where viscosity controls the interactions and flow properties. That local inhibition of the actin cytoskeleton eliminates anterior elongation suggests that



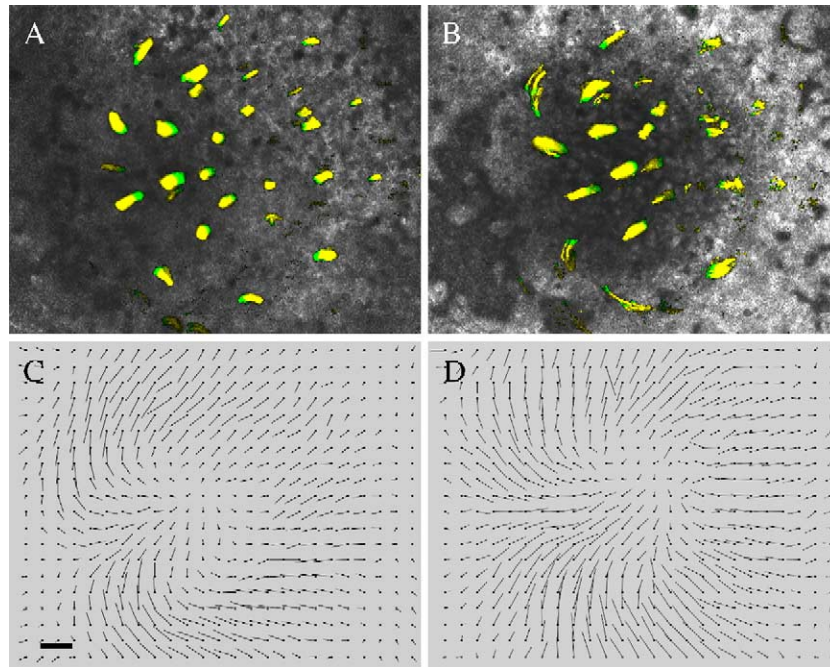


Fig. 6. Inhibition of cell movement in the presence of aphidicolin. Trajectories of DiI-labelled cells and vector velocity fields, showing the failure of streak formation and development in the absence of cell division. (A, B) Cell flow patterns revealed by DiI injection in embryo treated with aphidicolin. Labelled tracks show cell movement during the last 240 min before we took the brightfield images at 360 min (A) and 640 min (B) after the start of recording. The green heads of the tracks show cell movement during the last 60 min. (C, D) Vector velocity fields calculated for the images shown in panels (A, B). The initial vector flow field shows that the streak starts to form but stops since, in the absence of cell division, cells from the anterior and lateral *area pellucida* all move inward towards the centre of the embryo. No cells move anteriorly unlike normal development (Figs. 1–3). The white scale bar in panel (A) represents 250  $\mu\text{m}$ , the black scale bar in panel (C) corresponds to a velocity of 1  $\mu\text{m}/\text{min}$ . See also supplementary material movie 8.

extension of the anterior part of the forming streak requires active migration of the cells in the tip of the streak. Cells in the tip of the streak might chemotax up a gradient of a chemo-attractant (Painter et al., 2000). Blocking cell movement at the base of the streak, essentially at the meeting point of bifurcating cell flows, blocks both anterior and posterior streak extension, strongly suggesting that cell flow towards the meeting point is absolutely necessary for streak formation and elongation. The bifurcating flow pattern at the base of the streak resembles that seen during convergent extension in *Xenopus* and zebrafish embryos (Glickman et al., 2003; Keller et al., 2000).

The cell-flow patterns observed during streak formation strikingly parallel movements D'Amico and Cooper recently described for nuclei in the syncytial yolk layer in early gastrulation-stage fish embryos (D'Amico and Cooper, 2001). These nuclei also form two large-scale counter-rotating vortices flowing in a dorso-anterior direction, circulating around two quiescent lateral centres and merging at the midline of the embryo. They persist until the first somite stage. Thus, counter-rotating flows do not need active cell rearrangement but can occur in a cellular syncytium, where they may either involve active transport of nuclei along a microtubule network or result from flows in the cytoplasm. Epiboly in fish also seems to involve tissue flows directed towards the central midline with a flow bifurcation in the anterior and

posterior directions (Glickman et al., 2003). However, the extent to which these nuclear movements in the yolk syncytial layer resemble movements in the fish epiblast is not clear.

#### *Cell division is necessary for but does not drive streak formation*

Localised or oriented cell divisions could locally expand the cell mass in the epiblast, displacing cells at other locations. However, our experiments with aphidicolin showed clearly that the initial cell flows preceding streak formation occurred in the absence of cell division. A streak started to form; however, both the anterior and posterior extension stopped before streak formation was completed. During streak formation (even in the presence of aphidicolin), the tissue thickens at the site of the streak, as the darkening of the structure in the brightfield images indicates. Thus, rather than cell division, the active aggregation of cells at this site (seen clearly in the tracks of DiI-labelled cells and in the velocity profile, Fig. 6), which requires the recruitment of cells from neighbouring areas in the epiblast, drives thickening. Recruitment requires the epiblast to expand in surface area, which most likely involves the increased cell division we observed in the boundary region between the *area opaca* and *area pellucida* (Figs. 5B, E). Aphidicolin inhibition of



cell division prevents this expansion, so the flow of cells from anterior and lateral epiblast regions towards the location of streak formation thins and finally ruptures the epiblast. Thus, cell division in the early epiblast plays an essential permissive role in streak formation, expanding the surface area of the epiblast, in a functional analogue to the radial intercalation which increases the surface area of the ectoderm during gastrulation in *Xenopus* (Keller et al., 2000). We still must determine which signals coordinate the spatial pattern and dynamic changes of cell division during early stage gastrulation.

#### *The fate of cells moving in the epiblast*

What function do the cell flows during streak formation serve? What is the fate of the cells in various parts of the epiblast? The cells that will form the streak were derived from those cells just anterior to and overlaying Koller's sickle, which express many distinct genes: notably, *Wnt8c*, *nodal*, and *FGF8* (Chapman et al., 2002; Lawson et al., 2001). Our observations show that cells from the anterior–lateral epiblast replace the cells of Koller's sickle that move into the streak. A thin semicircle of cells at the posterior margin of the epiblast express *ephrinB3* (Baker and Antin, 2003; Baker et al., 2001). Between stages HH 2 and HH 4, *ephrinB3* transcription restricts to the anterior primitive streak until at HH 4 only Hensen's node expresses *ephrinB3*. Expression in the node continues until stage HH 10. According to the fate map of the early epiblast, many of the antero-lateral, *ephrinB3*-expressing cells end up in the lateral plate mesoderm (Hatada and Stern, 1994). Therefore, cell flows could cause this remarkable change in gene expression, and the confinement of expression to Hensen's node could result from the more lateral cells switching off *ephrinB3* expression once they invaginate. We must check whether *ephrinB3* helps control global epiblast movements.

Cells anterior to Koller's sickle move anteriorly. Central cells move in the anterior direction, while more lateral cells move first anteriorly then laterally. When we compare these movement patterns to the fate map of the epiblast at early stages of development, we find that anterior-moving cells join the neuro-ectoderm and surface ectoderm (Hatada and Stern, 1994). The flows may also account for dynamic changes in gene expression during early development of the neural plate, for instance, in the expression of *FGF* receptors 1 and 3 (Walshe and Mason, 2000). Though the position of the cells at the quiescent centres of the two vortices (Figs. 2A, C) does not correspond with any identified gene expression pattern, the fate map suggests that these cells will form epidermis. The cells that move posterior will contribute to extra-embryonic structures and contribute to the developing haemopoietic system. We have found that the cells in the posterior forming streak express *VegfA* and *VegfR2* (M. Chuai, X. Yang, and C.J. Weijer, in preparation).

#### *Possible mechanisms underlying streak formation*

Major open questions regarding streak formation are: what are the cellular mechanisms which cause the cell and tissue motions which produce the streak and which signals control them? Early streak formation could involve intercalation of cells in Koller's sickle at the base of the forming streak, driving bidirectional extension along the future anterior–posterior axis (Keller et al., 2003). In *Xenopus*, convergent extension involves intercalation of bipolar cells, and convergent extension occurs in Keller explants, isolated pieces of dorsal tissue (Keller et al., 2000; Wallingford et al., 2002). The Wnt mediated planar polarity signalling pathway, with Rho kinase as one of its downstream targets (Marlow et al., 2002) regulating convergent extension. However, the early chick epiblast does not seem to have bipolar cells (unpublished observations), and in our initial experiments, the Rho kinase inhibitor Y27632 did not inhibit early streak formation, even at concentrations which inhibited streak regression (Wei et al., 2001). Our latrunculin experiments (Fig. 4) show that the tip of the streak has to move forward actively, so streak formation must depend on more than just intercalation at the base of the streak. The planar polarity pathway also controls the cell–cell intercalation which drives germ band formation in *Drosophila* via preferential non-muscle-myosin-mediated contraction of cell boundaries perpendicular to the axis of extension. The pair rule genes then control the extension of boundaries in the direction of elongation, which locally reshuffles cells and extends the germ band (Bertet et al., 2004; Zallen and Wieschaus, 2004). We are now observing streak extension at higher magnification to look for consistent patterns of local cell rearrangement or polarisation in the chick epiblast.

Cells could also move in response to chemo-attractants/repellents. The cells in Koller's sickle could aggregate towards the dorsal midline in response to a chemo-attractant that these cells themselves produce, resulting in their aggregation at the ventral meeting point. The cells at the tip of the forming streak could then acquire the ability to respond to a gradient of another chemo-attractant, for instance, one that all cells in the epiblast produced, resulting in their movement towards the midline of the embryo. Alternatively, a signal coming from the base of the streak could repel the cells. Possible candidate molecules include the *FGFs* since epiblast cells express both *FGF* receptors and some *FGFs* from an early stage and we have recently shown that mesoderm cells chemotax to *FGF* (Karabagli et al., 2002; Walshe and Mason, 2000; Yang et al., 2002).

In this scenario, most cells move actively, probably on a basement membrane underlying the epiblast (Czirok et al., 2004) making cryptic filopodia in the direction of migration (Farooqui and Fenteany, 2005). We are now investigating this possibility.

Cells in the epiblast might also respond to signals which the endoblast emits while it is replacing the hypoblast in a

posterior–anterior direction. Hypoblast removal results in defective streak extension, and hypoblast rotation bends the streak (Azar and Eyal-Giladi, 1981; Bertocchi and Stern, 2002; Foley and Stern, 2001). The signal from the hypoblast could polarise the cells, resulting in anterior movement and rotational cell flows analogous to the counter-rotating fluid flows known as Raleigh–Bénard convection rolls in a fluid heated between two plates (Bodenschatz et al., 2000). The biological equivalent of the temperature gradient would be the hypoblast signal that polarises cells movement.

## Acknowledgments

We thank Dirk Dorman for advice on imaging. C.C. acknowledges a predoctoral training grant from the Center for Applied Mathematics at the University of Notre Dame. J.A.G. acknowledges NSF grant IBN-0083653, NASA grant NAG 2-1619, a PTL fellowship, an IBM Innovation Institute award, and support from the Interdisciplinary Center for the Study of Biocomplexity at the University of Notre Dame and the Biocomplexity Institute and the College of Arts and Sciences at Indiana University. C.J.W. acknowledges grants from the BBSRC and Wellcome Trust.

## Appendix A. Supplementary data

Supplementary data associated with this article can be found, in the online version, at [doi:10.1016/j.ydbio.2005.04.021](https://doi.org/10.1016/j.ydbio.2005.04.021).

## References

- Azar, Y., Eyal-Giladi, H., 1981. Interaction of epiblast and hypoblast in the formation of the primitive streak and the embryonic axis in chick, as revealed by hypoblast-rotation experiments. *J. Embryol. Exp. Morphol.* 61, 133–144.
- Bachvarova, R.F., Skromne, I., Stern, C.D., 1998. Induction of primitive streak and Hensen's node by the posterior marginal zone in the early chick embryo. *Development* 125, 3521–3534.
- Baker, R.K., Antin, P.B., 2003. Ephs and ephrins during early stages of chick embryogenesis. *Dev. Dyn.* 228, 128–142.
- Baker, R.K., Vanderboom, A.K., Bell, G.W., Antin, P.B., 2001. Expression of the receptor tyrosine kinase gene EphB3 during early stages of chick embryo development. *Mech. Dev.* 104, 129–132.
- Bertet, C., Sulak, L., Lecuit, T., 2004. Myosin-dependent junction remodelling controls planar cell intercalation and axis elongation. *Nature* 429, 667–671.
- Bertocchi, F., Stern, C.D., 2002. The hypoblast of the chick embryo positions the primitive streak by antagonizing nodal signaling. *Dev. Cell* 3, 735–744.
- Bodenschatz, E., Pesch, W., Ahlers, G., 2000. Recent developments in Rayleigh-Bernard Convection. *Ann. Rev. Fluid Mech.* 32, 708–778.
- Chapman, S.C., Collignon, J., Schoenwolf, G.C., Lumsden, A., 2001. Improved method for chick whole-embryo culture using a filter paper carrier. *Dev. Dyn.* 220, 284–289.
- Chapman, S.C., Schubert, F.R., Schoenwolf, G.C., Lumsden, A., 2002. Analysis of spatial and temporal gene expression patterns in blastula and gastrula stage chick embryos. *Dev. Biol.* 245, 187–199.
- Chapman, S.C., Brown, R., Lees, L., Schoenwolf, G.C., Lumsden, A., 2004. Expression analysis of chick Wnt and frizzled genes and selected inhibitors in early chick patterning. *Dev. Dyn.* 229, 668–676.
- Concha, M.L., Adams, R.J., 1998. Oriented cell divisions and cellular morphogenesis in the zebrafish gastrula and neurula: a time-lapse analysis. *Development* 125, 983–994.
- Czirok, A., Rongish, B.J., Little, C.D., 2004. Extracellular matrix dynamics during vertebrate axis formation. *Dev. Biol.* 268, 111–122.
- D'Amico, L.A., Cooper, M.S., 2001. Morphogenetic domains in the yolk syncytial layer of axiating zebrafish embryos. *Dev. Dyn.* 222, 611–624.
- Eyal-Giladi, H., Kochav, S., 1976. From cleavage to primitive streak formation: a complementary normal table and a new look at the first stages of the development of the chick: I. General morphology. *Dev. Biol.* 49, 321–337.
- Farooqui, R., Fenteany, G., 2005. Multiple rows of cells behind an epithelial wound edge extend cryptic lamellipodia to collectively drive cell-sheet movement. *J. Cell Sci.* 118, 51–63.
- Foley, A.C., Stern, C.D., 2001. Evolution of vertebrate forebrain development: how many different mechanisms? *J. Anat.* 199, 35–52.
- Foley, A.C., Skromne, I., Stern, C.D., 2000. Reconciling different models of forebrain induction and patterning: a dual role for the hypoblast. *Development* 127, 3839–3854.
- Glickman, N.S., Kimmel, C.B., Jones, M.A., Adams, R.J., 2003. Shaping the zebrafish notochord. *Development* 130, 873–887.
- Gong, Y., Mo, C., Fraser, S.E., 2004. Planar cell polarity signalling controls cell division orientation during zebrafish gastrulation. *Nature*.
- Graeper, L., 1929. Die Primitiventwicklung des Hühnchens nach stereokinematographischen Untersuchungen kontrolliert durch vitale Farbmarmkierung und verglichen mit der Entwicklung anderer Wirbeltiere. *Wilhelm Roux' Arch. Entwicklungsmech. Org.* 116, 382–429.
- Hamburger, V., Hamilton, H.L., 1992. A series of normal stages in the development of the chick embryo: 1951. *Dev. Dyn.* 195, 231–272.
- Hatada, Y., Stern, C.D., 1994. A fate map of the epiblast of the early chick embryo. *Development* 120, 2879–2889.
- Karabagli, H., Karabagli, P., Ladher, R.K., Schoenwolf, G.C., 2002. Comparison of the expression patterns of several fibroblast growth factors during chick gastrulation and neurulation. *Anat. Embryol. (Berl.)* 205, 365–370.
- Keller, R., Davidson, L., Edlund, A., Elul, T., Ezin, M., Shook, D., Skoglund, P., 2000. Mechanisms of convergence and extension by cell intercalation. *Philos. Trans. R. Soc. Lond., Ser. B Biol. Sci.* 355, 897–922.
- Keller, R., Davidson, L.A., Shook, D.R., 2003. How we are shaped: the biomechanics of gastrulation. *Differentiation* 71, 171–205.
- Lawson, A., Schoenwolf, G.C., 2001. Cell populations and morphogenetic movements underlying formation of the avian primitive streak and organizer. *Genesis* 29, 188–195.
- Lawson, A., Colas, J.F., Schoenwolf, G.C., 2001. Classification scheme for genes expressed during formation and progression of the avian primitive streak. *Anat. Rec.* 262, 221–226.
- Marlow, F., Topczewski, J., Sepich, D., Solnica-Krezel, L., 2002. Zebrafish Rho kinase 2 acts downstream of Wnt11 to mediate cell polarity and effective convergence and extension movements. *Curr. Biol.* 12, 876–884.
- Michael, W.M., Newport, J., 1998. Coupling of mitosis to the completion of S phase through Cdc34-mediated degradation of Wee1. *Science* 282, 1886–1889.
- Painter, K.J., Maini, P.K., Othmer, H.G., 2000. A chemotactic model for the advance and retreat of the primitive streak in avian development. *Bull. Math. Biol.* 62, 501–525.
- Sanders, E.J., Varedi, M., French, A.S., 1993. Cell proliferation in the gastrulating chick embryo: a study using BrdU incorporation and PCNA localization. *Development* 118, 389–399.
- Shah, S.B., Skromne, I., Hume, C.R., Kessler, D.S., Lee, K.J., Stern, C.D., Dodd, J., 1997. Misexpression of chick Vgl in the marginal zone induces primitive streak formation. *Development* 124, 5127–5138.

- Siegert, F., Weijer, C.J., Nomura, A., Miike, H., 1994. A gradient method for the quantitative analysis of cell movement and tissue flow and its application to the analysis of multicellular Dictyostelium development. *J. Cell Sci.* 107, 97–104.
- Skromne, I., Stern, C.D., 2001. Interactions between Wnt and Vg1 signalling pathways initiate primitive streak formation in the chick embryo. *Development* 128, 2915–2927.
- Skromne, I., Stern, C.D., 2002. A hierarchy of gene expression accompanying induction of the primitive streak by Vg1 in the chick embryo. *Mech. Dev.* 114, 115–118.
- Vakaet, L., 1970. Cinephotomicrographic investigations of gastrulation in the chick blastoderm. *Arch. Biol. (Liege)* 81, 387–426.
- Waddington, C.H., 1932. Experiments on the development of chick and duck embryos cultivated in vitro. *Philos. Trans. R. Soc. Lond., B* 221, 179–230.
- Waddington, C.H., 1933. Induction by the primitive streak and its derivatives in the chick. *J. Exp. Biol.* 10, 38–48.
- Wallingford, J.B., Fraser, S.E., Harland, R.M., 2002. Convergent extension: the molecular control of polarized cell movement during embryonic development. *Dev. Cell* 2, 695–706.
- Walshe, J., Mason, I., 2000. Expression of FGFR1, FGFR2 and FGFR3 during early neural development in the chick embryo. *Mech. Dev.* 90, 103–110.
- Wei, Y., Mikawa, T., 2000. Formation of the avian primitive streak from spatially restricted blastoderm: evidence for polarized cell division in the elongating streak. *Development* 127, 87–96.
- Wei, L., Roberts, W., Wang, L., Yamada, M., Zhang, S., Zhao, Z., Rivkees, S.A., Schwartz, R.J., Imanaka-Yoshida, K., 2001. Rho kinases play an obligatory role in vertebrate embryonic organogenesis. *Development* 128, 2953–2962.
- Yang, X., Dormann, D., Munsterberg, A.E., Weijer, C.J., 2002. Cell movement patterns during gastrulation in the chick are controlled by positive and negative chemotaxis mediated by FGF4 and FGF8. *Dev. Cell* 3, 425–437.
- Zallen, J.A., Wieschaus, E., 2004. Patterned gene expression directs bipolar planar polarity in *Drosophila*. *Dev. Cell* 6, 343–355.